IEEE Access
Multidisciplinary ⋮ Rapid Review ⋮ Open Access Journal

Received 3 April 2023, accepted 28 April 2023, date of publication 1 May 2023, date of current version 22 May 2023.

Digital Object Identifier 10.1109/ACCESS.2023.3272044

RESEARCH ARTICLE

Phase Rotation Approach With Mixed-Numerology Architecture for PAPR Reduction in 5G and Beyond

AHMET ENES DURANAY[1], EBUBEKIR MEMISOGLU[1], BAŞAK ÖZBAKIŞ[2], AND HÜSEYIN ARSLAN[1], (Fellow, IEEE)

[1]Department of Electrical and Electronics Engineering, Istanbul Medipol University, 34810 Istanbul, Turkey
[2]Department of Research and Development, Vestel Electronics, 45030 Manisa, Turkey

Corresponding author: Ahmet Enes Duranay (aeduranay@medipol.edu.tr)

This work was supported by the Scientific and Technological Research Council of Turkey (TÜBİTAK), with the cooperation of VESTEL and Istanbul Medipol University, under Grant 5200030.

ABSTRACT For a wide range of service requirements, the 5G-NR offers significant flexibility based on OFDM with numerous numerologies. However, OFDM is recognized to have a significant disadvantage due to a high PAPR. On the other hand, the PAPR reduction for mixed-numerology OFDM has received little attention compared to single-numerology OFDM, despite there being possible challenges and advantages such as computational complexity and new structure opportunity, respectively. In this paper, the phase rotation PAPR reduction approach on mixed-numerology OFDM is proposed for the first time. Unlike the single-numerology approach, the need for additional IFFT and side information overhead is eliminated, and the mixed-numerology transmitter structure is exploited to provide three novel approaches, namely proposed numerology-based (Proposed-NB), proposed symbol-based (Proposed-SB), and proposed location-based (Proposed-LB). Proposed-NB has the same PAPR performance with a lower complexity compared to the partial transmit sequence (PTS) method for single-numerology OFDM. Moreover, the new ability to use multiple phase factors for the same numerology symbols in the defined largest symbol length enhances the PAPR reduction performance further using Proposed-SB. While all symbols are jointly optimized in the Proposed-SB, Proposed-LB drives a sub-optimal solution developed by optimizing the selected symbols. Due where the presence of different symbols duration between numerologies and also consecutive symbols in the same numerology, PAPR reduction performance in Proposed-LB almost reaches the optimum Proposed-SB performances with a lower computational complexity compared to Proposed-SB. The conducted numerical results validate the superiority of the proposed methods for 5G and beyond compared to PTS and numerology scheduling methods.

INDEX TERMS Fifth generation-new radio (5G-NR) and beyond, orthogonal frequency division multiplexing (OFDM), peak-to-average power ratio (PAPR), mixed numerologies, phase rotation, partial transmit sequence (PTS).

I. INTRODUCTION

Fifth generation-New Radio (5G-NR) needs to provide the necessary flexibility to support its diverse requirements and use cases [1]. This is achieved by the introduction of multiple numerologies, where numerology refers to the set of parameters such as subcarrier spacing, symbol length, and cyclic prefix (CP) of the orthogonal frequency division multiplexing (OFDM) signals [2]. Despite OFDM's widespread adoption (and the consequent backward compatibility), it suffers from various issues such as a high peak-to-average power ratio (PAPR), leading to signal distortion caused by the power amplifier operating in its non-linear region [3].

The PAPR is a well-known problem in single-numerology OFDM systems [4]. Accordingly, it has been studied extensively. Iterative-cancellation and filtering (ICF) technique

The associate editor coordinating the review of this manuscript and approving it for publication was Julien Le Kernec.

clips the signal to maintain PAPR below a certain threshold, but clipping causes in-band and out-of-band radiation which in turn requires filtering and also exacerbates bit error rate (BER) problems [5]. In frequency-domain spectral shaping (FDSS), the symmetric spectral extension is added and then filtered for shaping, but this also affects the demodulation reference signals, which is undesirable [6]. In selected mapping (SLM), the input symbols are multiplied by different random phase sequences, each of which is then passed through the inverse fast Fourier transform (IFFT) operation [7]. Then, the signal with the lowest PAPR is selected and used for transmission. In partial transmit sequence (PTS), the bandwidth is divided into subbands. After the IFFT operation for each subband, the time domain signal for each is rotated with different phase factors to minimize PAPR [8]. PTS is a distortion-free approach that reduces the PAPR without any deformation to the transmitted signals; as a result, it has no impact on the BER performance [9]. Although PTS is a promising PAPR reduction technique for OFDM, this method introduces an increased computational complexity by optimizing phase factors and performing IFFT operation for each subband at the transmitter [10]. Furthermore, side information (SI) that includes subbands and phase factors is necessary to be shared with the receiver and causes overhead.

Unlike single-numerology OFDM, the PAPR reduction for mixed numerologies is not well-investigated in the literature. In fact, only a handful of works [11], [12], [13], [14], [15] have tried to address this issue. The ICF approach is applied for PAPR reduction in [11] and [12] while considering inter-numerology interference (INI). In [13], power allocation is optimized between different numerologies to reduce PAPR. In [14], PAPR reduction is achieved using noise shaped ICF where the alternating direction of multipliers is optimized. Lastly, [15] presents a numerology scheduling strategy for both time and frequency domain numerology multiplexing to reduce PAPR.

PAPR reduction for mixed numerology OFDM needs further research considering other approaches in the literature [16]. Also, none of the above approaches make use of the structure of mixed-numerology transmitters, which are inherently more complicated compared to conventional single-numerology transmitters [17]. It is, therefore, important to devise low-complexity PAPR reduction schemes to avoid additional complexity for the mixed-numerology transceivers.

Accordingly, in this work, a PAPR reduction method with a phase rotation approach is proposed for the first time by utilizing mixed-numerology architecture where the time domain signals of mixed-numerology OFDM are multiplied with phase factors before the summation of the signals. Here, the multiplication of phase factors is applied differently for three proposed methods: numerology-based, symbol-based, and location-based PAPR reduction. The numerology-based method (Proposed-NB) multiplies the time domain signal of each numerology with a different phase factor. In contrast, the novel symbol-based method (Proposed-SB) multiplies the

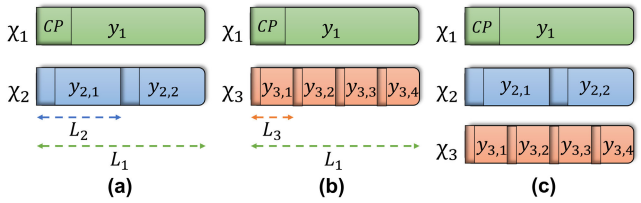

FIGURE 1. The symbols of mixed numerologies in the time domain for the scenarios (a) χ_1&χ_2, (b) χ_1&χ_3, and (c) χ_1&χ_2&χ_3.

CP-OFDM symbols with a different phase factor. Moreover, a location-based method (Proposed-LB) is developed as a novel sub-optimal solution, which exploits the highest signals peak power and provides self-dependence in PAPR reduction between symbols with lower computational complexity. Proposed methods neither require additional IFFT processes at the transmitter nor recovery with SI at the receiver. The performance of the proposed methods has been evaluated for different mixed-numerology scenarios and phase factors, and it is shown by numerical results that a better PAPR reduction performance and lower computational complexity are achieved compared to conventional PTS in single numerology [18] and numerology scheduling technique in mixed numerologies [15].

The rest of this paper is organized as follows. Section II explains the general system model of CP-OFDM mixed-numerology transmission. The proposed PAPR reduction methods are described in Section III. The analysis for computational complexity is also included in this section. The numerical simulation results and analysis are given in Section IV. Lastly, Section V provides a conclusion.

Notations: Throughout the paper, a, $\mathbf{a}$, $\overline{x}$, $\hat{x}$, and the superscript of (s) denote the complex number, the complex vector, the optimum x, the estimated x and the s^{th} search case, respectively. The notations $E[.]$, $[.]^T$, $\lfloor\cdot\rfloor$, and $\wedge$ represent expectation, transpose, floor, and logical-and operations, respectively. $\mathbb{Z}^+$, $\exists$, and $\in$ refer to positive integers, the existence of a variable, and a member of the set, respectively.

II. SYSTEM MODEL

In this section, mixed-numerology transmission is introduced. In 5G-NR mixed-numerology systems, at most three different numerologies can be multiplexed over a band and CP-OFDM symbols are aligned over the least common multiplier (LCM) symbol duration, as illustrated in Fig. 1 [2].

In the system model, the modulated symbols to be sent over a bandwidth (B) are divided into $I \in \mathbb{Z}^+$ bandwidth parts (BWPs), and the i^{th} numerology is assigned to each BWP where $i = 1, 2, .., I$. Numerology, IFFT size, CP length, CP-OFDM symbol length, and subcarrier spacing for the i^{th} numerology are denoted by χ_i, N_i, L_i^{CP}, $L_i = N_i + L_i^{CP}$, and $\Delta f_i = 15 \cdot 2^p$ kHz with an integer value p, respectively.

After mapping the bits into complex symbols with an average unit power, the symbol vector $\mathbf{X}_{i,m_i} \in \mathbb{C}^{N_i \times 1}$ in the frequency domain is obtained, where $m_i = 1, 2, \ldots, M_i$ denotes the OFDM symbol index of χ_i and $M_i = \Delta f_i/(15 \cdot 10^3) = 2^p$. With the use of N_i-point IFFT, the discrete

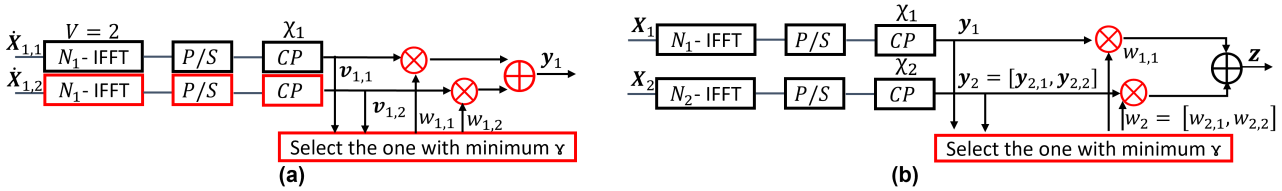

FIGURE 2. (a) The transmitter block diagram of PTS with V=2 for χ_1 and (b) proposed methods for χ_1&χ_2 mixed-numerology scenario where $w_{2,1} = w_{2,2}$ for Proposed-NB. The red color indicates the required additional operation only for the PAPR reduction.

time-domain signal $\mathbf{y}_{i,m_i}$ can be expressed as

$$y_{i,m_i}(n) = \sqrt{\frac{\eta_i}{N_i}} \sum_{k=0}^{K_i-1} X_{i,m_i}(k) e^{\frac{j2\pi\left(n-L_i^{CP}\right)(k+\Delta k_i)}{N_i}}, \quad 0 \le n \le L_i - 1, \tag{1}$$

where K_i is the total number of subcarriers assigned for the i^{th} numerology, Δk_i is the subcarrier index of the i^{th} BWP frequency shift, and η_i is the power scaling factor.

The CP-OFDM symbols structures of mixed numerologies in the time domain for different scenarios are shown in Fig. 1 where $\Delta f_1 = 15$ kHz, $\Delta f_2 = 30$ kHz, and $\Delta f_3 = 60$ kHz. The scenario of χ_2&χ_3 is not considered in this study since it has the same structure and thus the same performance gains as χ_1&χ_2 due to fact that $\Delta f_2/\Delta f_1 = \Delta f_3/\Delta f_2$. The OFDM symbols of χ_i by the provision of $L = L_i M_i$ length are concatenated where L is the length of an LCM symbol. The time domain signal can be shown as

$$\mathbf{y}_i = \left[\mathbf{y}_{i,1}{}^T, \mathbf{y}_{i,2}{}^T, \ldots, \mathbf{y}_{i,M_i}{}^T\right]^T. \tag{2}$$

Then, the composite time domain signal of the mixed-numerology OFDM $\mathbf{z} \in \mathbb{C}^{L\times 1}$ with a unit power is generated by summing all $\mathbf{y}_i$'s as $\mathbf{z} = \mathbf{y}_1 + \mathbf{y}_2 + \cdots + \mathbf{y}_I$. Afterwards, it passes through the power amplifier (PA) prior to transmission by an antenna.

III. PROPOSED PHASE FACTOR METHODS FOR MIXED NUMEROLOGIES

In this section, a brief description of the benchmark PTS technique is given. Then, the proposed methods are explained including a computational complexity analysis.

A. PARTIAL TRANSMIT SEQUENCE (PTS) METHOD

Partial Transmit Sequence (PTS) splits the input symbol vector $\dot{\mathbf{X}}_i = \left[\dot{\mathbf{X}}_{i,1}^T, \dot{\mathbf{X}}_{i,2}^T, \ldots, \dot{\mathbf{X}}_{i,V}^T\right]^T$ into V disjoint subblocks, where the $\dot{\mathbf{X}}_{i,k}$ are symbol subsequences in frequency-domain and $k \in \{1, 2, \ldots, V\}$ [8]. The $\dot{\mathbf{X}}_{i,k}$ are transformed to the time domain using IFFT, and $\dot{\mathbf{v}}_{i,k}$ can be shortly expressed as

$$\dot{\mathbf{v}}_{i,k} = \text{IFFT}\{\dot{\mathbf{X}}_{i,k}\}, \tag{3}$$

where generated V subblocks are equal in length [18]. Then, followed by CP insertion to $\dot{\mathbf{v}}_{i,k}$, $\mathbf{v}_{i,k}$ is finally obtained. As shown in Fig. 2 (a), each portioned subblock $\mathbf{v}_{i,k}$ is multiplied by all combinations of the complex phase factors. The phase factors are chosen from a given weighting cluster, and the size of the cluster is defined by W. PTS requires $S^{PTS} = W^{V-1}$ numbers of phase searches. After shifting the phases of the partitions, the $\overline{w}_{i,k}$ phases are obtained to minimize the PAPR value [19]. Then, the selected $\overline{\mathbf{y}}_\mathbf{i}$ from all generated signals is written as

$$\overline{\mathbf{y}}_i = \sum_{k=1}^{V} \overline{w}_{i,k} \mathbf{v}_{i,k}. \tag{4}$$

B. PROPOSED METHODS

This section describes the proposed methods under different titles for the optimal solutions as the Proposed-NB and Proposed-SB and the sub-optimal solution as Proposed-LB, respectively.

1) PROPOSED-NB AND PROPOSED-SB

The phase rotation approach is developed by exploiting the mixed-numerology OFDM transmitter structure of the 5G-NR rather than adding V blocks for each numerology. In Fig. 2 (b), the simplified transmitter block diagram of the proposed methods is presented. Some known initial processes are omitted in the figure such as serial-to-parallel (S/P) conversion and subcarrier mapping (SM) [20].

The proposed methods take place after the CP addition for each χ_i. To obtain the minimum PAPR value of the composite signal $\mathbf{z}$, the optimum phases $\overline{w}_{i,m_i}$ are found for the M_i symbols in each numerology χ_i.

The PAPR reduction problem to obtain optimum composite signal $\overline{\mathbf{z}}$ can be represented as

$$\overline{\mathbf{z}} = \min_s \left(\max_{0\le n\le L-1} \left| z(n)^{(s)} \right| \right), \tag{5}$$

where the superscript (s) represents a phase search case. The s^{th} composite signal $\mathbf{z}^{(s)}$ can be generated from the summation of signals $\mathbf{y}_i^{(s)}$ as

$$\mathbf{z}^{(s)} = \sum_{i=1}^{I} \mathbf{y}_i^{(s)}. \tag{6}$$

Similar to the conventional mixed-numerology transmission, the derived signal $\mathbf{y}_i^{(s)}$ is as follows:

$$\mathbf{y}_i^{(s)} = \left[\mathbf{y}_{i,1}^{(s)T}, \mathbf{y}_{i,2}^{(s)T}, \ldots, \mathbf{y}_{i,M_i}^{(s)\ T}\right]^T. \tag{7}$$

$\mathbf{y}_i^{(s)}$ is formed by concatenating time domain symbols $\mathbf{y}_i$, as given in (2), and multiplied by the phase factors. As an illustration, the proposed method for χ_1&χ_2 mixed-numerology scenario where $\Delta f_1 = 15$ kHz and $\Delta f_2 =$

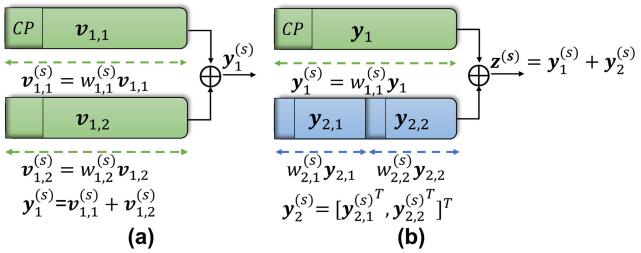

FIGURE 3. (a) The execution of the PTS with V=2 for χ_1 and (b) the proposed method for the χ_1&χ_2 mixed-numerology scenario.

30 kHz is depicted in Fig. 3 (b). Also, PTS with V = 2 for χ_1 is shown in Fig. 3 (a) for the comparison of the methods.

With the phase of corresponding rotation factor $w_{i,m_i}^{(s)}$, the rotated $\mathbf{y}_{i,m_i}^{(s)}$ can be found as

$$\mathbf{y}_{i,m_i}^{(s)} = w_{i,m_i}^{(s)} \mathbf{y}_{i,m_i}, \tag{8}$$

where $w_{i,m_i}^{(s)}$ is the phase factor for the i^{th} numerology and m^{th} symbol of the $\mathbf{y}_{i,m_i}$ time domain signal. The phase factor w_{i,m_i} is given as

$$w_{i,m_i} = e^{j2\pi r/W}, \quad r \in \{0, 1, \ldots, W-1\}. \tag{9}$$

Two main phase rotation approaches and one sub-optimal method are proposed for PAPR reduction in mixed numerologies. The phase rotation operation is performed differently for the proposed methods. In Proposed-NB, a numerology-based calculation is implemented and the phase rotation is applied on $\mathbf{y}_i$. In other words, a single phase is used for all $\mathbf{y}_{i,m_i}$'s in the i^{th} numerology, i.e., $w_{i,1}^{(s)} = w_{i,2}^{(s)} = \cdots = w_{i,M_i}^{(s)}$. However, at this point, the phase rotation is applied distinctively on the $\mathbf{y}_{i,m_i}$ in the novel Proposed-SB. Therefore, for the s^{th} search case, the w_{i,m_i} factor can be chosen differently for each $\mathbf{y}_{i,m_i}$ in Proposed-SB. Accordingly, Proposed-NB and Proposed-SB require

$$S^{NB} = W^{I-1} \tag{10}$$

and

$$S^{SB} = W^{\left(\sum_{i=1}^{I} M_i\right)-1} \tag{11}$$

numbers of phase searches, respectively. Therefore, the phase search case is defined as $s \in \{1, 2, \ldots, S^{NB}\}$ for Proposed-NB and $s \in \{1, 2, \ldots, S^{SB}\}$ for Proposed-SB.

The digital processes of the mixed-numerology transmitter block diagram are practically adapted to decrease PAPR (γ) for $\mathbf{z}$. Then, the PAPR for the s^{th} case is calculated by

$$\gamma^{(s)} = \frac{\max\limits_{0 \le n \le L_i - 1} \left|z(n)^{(s)}\right|^2}{E\left[\left|z(n)^{(s)}\right|^2\right]}, \tag{12}$$

where E[·] denotes the expectation operation. The proposed methods require finding the optimum set of phases to obtain minimum γ. The optimum phases $\overline{w}_{i,m_i}$ can be found as

$$\overline{w}_{i,m_i} = \arg\min_{w_{i,m_i}^{(s)}} \left(\gamma^{(s)}\right), \tag{13}$$

Algorithm 1 The Main Proposed Phase Rotation Algorithm for PAPR Reduction of 5G and Beyond

```
Define B, I, χ_i and W
Compute y_{i,m_i} and y_i according to (1) and (2)
Generate the phase weighting cluster according to (9)
Decide the proposed method (Proposed-NB or Proposed-SB)
for s = 0 to S^NB (10) or S^SB (11) do
    Compute y_{i,m_i}^(s) according to (8)
    Compute y_i^(s) according to (7)
    Compute z^(s) according to (6)
    Compute γ^(s) according to (12)
end for
Find the optimum phases w̄_{i,m_i} by (13)
Select z̄ with the minimum γ value by (5)
```

where arg min finds the optimum phase factors for the signal with minimum PAPR on the s^{th} search case. Finally, the optimum composite signal $\overline{\mathbf{z}}$ corresponding to $\overline{w}_{i,m_i}$ is selected to transmit. The process flow for the proposed PAPR reduction technique is summarized in Algorithm 1.

The novel ability of the multiple phase factors (w_{i,m_i}) for the i^{th} numerology symbols in defined L length with Proposed-SB enables the design of sub-optimal solution considering the location of the highest signals peak power. In this process, the numerology χ_q is excluded from the phase multiplication process at the cost of meager PAPR degradation compared to the previous solution. χ_q can be defined as the numerology with the lowest subcarrier spacing in the system ($\chi_q = \chi_1$ for the considered scenarios) as

$$\Delta f_q = \min\left(\Delta f_i\right), \tag{14}$$

where q is an integer value. In this way, PAPR reduction between symbols ($\mathbf{y}_{i,m_i}$) of the same (i^{th}) numerology is achieved with any reliance on the numerology χ_q, rendering Proposed-SB self-dependent. Eventually, by the provision of LCM, the existence of different symbol durations between numerologies and also consecutive symbols in the same numerology provide the location-based PAPR reduction. From this approach, Proposed-LB is designed as a sub-optimal solution for Proposed-SB.

2) PROPOSED-LB

In Proposed-LB, the location of composite signal's ($\mathbf{z}(n)^{(s)}$) peak power ($\hat{n}^{(s)}$) is estimated firstly as

$$\hat{n}^{(s)} = \arg\max_{n} \left(\left|z(n)^{(s)}\right|^2\right), \tag{15}$$

where $0 \le n \le L_q$, and L_q is the CP-OFDM symbol length of the numerology with Δf_q subcarrier spacing.

L_{q+1} is the CP-OFDM symbol length of the numerology with the lowest subcarrier spacing after χ_q. The symbol-based phase rotation operation is applied only for each symbol within the L_{q+1} time duration where $\hat{n}^{(s)}$ exists. Therefore,

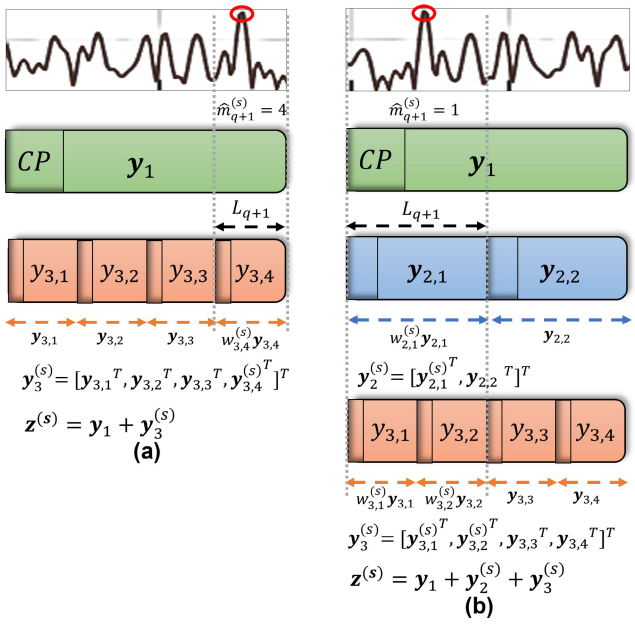

FIGURE 4. An instant execution of the Proposed-LB for the (a) χ_1&χ_3, and (b) the χ_1&χ_2&χ_3 mixed-numerology scenarios where the peak of signal power z taken placed at the last, and the second L_3 time period, respectively.

there is a need to detect considered L_{q+1} time duration after finding the index of the peak value. The index of the estimated time interval $\hat{m}_{q+1}^{(s)}$ where $\hat{n}^{(s)}$ is captured can be found as

$$\hat{m}_{q+1}^{(s)} = \left\lfloor \hat{n}^{(s)} / L_{q+1} \right\rfloor + 1. \tag{16}$$

Here, $1 \leq \hat{m}_{q+1}^{(s)} \leq M_{q+1}$ and $\lfloor \cdot \rfloor$ denotes the floor operation, which gives the greatest integer less or equal to the input value. After obtaining the $\hat{m}_{q+1}^{(s)}$, optimization of the phase rotation stage starts. However, the estimation of $\hat{n}^{(s)}$ and $\hat{m}_{q+1}^{(s)}$ proceed before every (s) phase rotation operation. Hence, (15) and (16) are cyclic processes.

An illustration of Proposed-LB is provided in Fig. 4 for the χ_1&χ_3 and χ_1&χ_2&χ_3 mixed-numerology scenarios. In order to reduce the cost of the complexity from phase optimization, phase searches are limited only to the single L_{q+1} time interval with $\hat{m}_{q+1}^{(s)}$ index. However, during the phase rotation process, the location of the peak value of the composite signal $(\hat{n}^{(s)})$ can move out from the considered L_{q+1} time interval. Then, it requires doing phase optimization on the another L_{q+1} time interval with different $\hat{m}_{q+1}^{(s)}$ index where different $\mathbf{y}_{i,m_i}$ symbols are set. Thus, $\mathbf{y}_{i,m_i}^{(s)}$ for Proposed-LB can be found in (17), as shown at the bottom of the page. The process flow for the proposed sub-optimal PAPR reduction technique with Proposed-LB is summarized in Algorithm 2.

Algorithm 2 The Sub-Optimal Algorithm for PAPR Reduction of 5G and Beyond

1: Define B, I, χ_i and W
2: Compute $\mathbf{y}_{i,m_i}$ and $\mathbf{y}_i$ according to (1) and (2)
3: Generate the phase weighting cluster according to (9)
4: Define χ_{q+1} numerology according to χ_q and (14)
5: **for** $s = 0$ **to** S^{LB} (18) **do**
6: Compute $\hat{n}^{(s)}$ according to (15)
7: Compute $\hat{m}_{q+1}^{(s)}$ according to (16)
8: Compute $\mathbf{y}_{i,m_i}^{(s)}$ according to (17)
9: Compute $\mathbf{y}_i^{(s)}$, $\mathbf{z}^{(s)}$, and $\gamma^{(s)}$ according to (7), (6), and (12)
10: **end for**
11: Find the optimum phases $\overline{w}_{i,m_i}$ by (13)
12: Select $\bar{\mathbf{z}}$ with the minimum γ value by (5)

The phase rotation operation is applied on $\mathbf{y}_{i,m_i}$ within L_{q+1} time interval with $\hat{m}_{q+1}^{(s)}$ index until $\hat{n}^{(s)}$ move to a time interval with another $\hat{m}_{q+1}^{(s)}$ index or $w_{i,m_i}^{(s)}$ in (9) reaches the s^{th} search case where $r = W - 1$ for all symbols within the considered time duration. Since Proposed-LB takes the PAPR problem as M_{q+1} different self-dependent phase rotation operations based on the position of the $\hat{n}^{(s)}$ and numerologies in the system, a certain number of phase searches for Proposed-LB can not be predefined in contrast to S^{SB}.

The total number of the required phase searches is given as S^{LB}, where the phase search case is defined as $s \in \{1, 2, \ldots, S^{LB}\}$ for Proposed-LB. S^{LB} is generated by summing all searched phase cases for each L_{q+1} time interval as

$$S^{LB} = \sum_{m_{q+1}=1}^{M_{q+1}} S_{m_{q+1}}^{LB}, \tag{18}$$

where the number of phase search cases for each L_{q+1} time interval is defined as $S_{m_{q+1}}^{LB}$ and $\exists S_{m_{q+1}}^{LB} . S_{m_{q+1}}^{LB} \in \mathbb{Z}^+ \wedge m_{q+1} = \hat{m}_{q+1}^{(s)}$.

The minimum number of the phase search case for S^{LB} is represented by S_{min}^{LB} as

$$S_{min}^{LB} = W^{\left(\left(\sum_{i=2}^{I} M_i\right)-1\right)/M_{q+1}}, \tag{19}$$

where $w_{i,m_i}^{(s)}$ in (9) reaches the s^{th} search case for $r = W-1$ for all symbols within the considered time duration. Phase rotation operation is only applied on a single time L_{q+1} interval and hence S_{min}^{LB} equals to $S_{m_{q+1}}^{LB}$ where $\hat{m}_{q+1}^{(s)} = k$ and k is a constant integer value for all (s) phase searches.

$$\mathbf{y}_{i,m_i}^{(s)} = \begin{cases} w_{i,m_{q+1}}^{(s)} \mathbf{y}_{i,m_{q+1}}, & m_{q+1} = \hat{m}_{q+1}^{(s)} \text{ and } \hat{m}_{q+1}^{(s)} \in \{1, \ldots, M_{q+1}\}, \quad i \in \{q+1\}, \\ w_{i,m_i}^{(s)} \mathbf{y}_{i,m_i}, & \frac{M_i}{M_{q+1}}\left(\hat{m}_{q+1}^{(s)} - 1\right) + 1 \leq m_i \leq \frac{M_i}{M_{q+1}} \hat{m}_{q+1}^{(s)} \text{ and } \quad \forall m_i,\ i \notin \{q, q+1\}. \end{cases} \tag{17}$$

On the other hand, the maximum number of the phase search case for S^{LB}, i.e., S^{LB}_{max} can occur in the scenario for the location of the highest signals peak power is moved to all other L_{q+1} time intervals ($\hat{m}^{(s)}_{q+1} = 1, \ldots, M_{q+1}$) while at the same time $w^{(s)}_{i,m_i}$ in (9) reaches the s^{th} search case for $r = W - 1$ for all time intervals. The S^{LB}_{max} can be found as follows:

$$\begin{aligned} S^{LB}_{max} &= S^{LB}_{min} + \left(S^{LB}_{min} - 1\right)\left(M_{q+1} - 1\right) \\ &= M_{q+1}\left(S^{LB}_{min} - 1\right) + 1 \\ &= M_{q+1}\left(W^{\left(\left(\sum_{i=2}^{I} M_i\right)-1\right)/M_{q+1}} - 1\right) + 1. \end{aligned} \tag{20}$$

Finally, S^{LB} is defined as an interval with $S^{LB}_{min} \leq S^{LB} \leq S^{LB}_{max}$ according to (19) and (20) as

$$W^{\frac{\left(\sum_{i=2}^{I} M_i\right)-1}{M_{q+1}}} \leq S^{LB} \leq M_{q+1}\left(W^{\frac{\left(\sum_{i=2}^{I} M_i\right)-1}{M_{q+1}}} - 1\right) + 1. \tag{21}$$

The PAPR is calculated depending on the OFDM symbol length by the provision of LCM L. The complementary cumulative distribution function (CCDF) of the PAPR is defined as [13]

$$CCDF(\gamma) \approx 1 - \exp\left(-\sqrt{\Lambda \cdot \gamma}\, e^{-\gamma}\right), \tag{22}$$

where

$$\begin{aligned} \Lambda &\triangleq \frac{L^2}{\Delta f_i^2 \pi}\left(\sum_{k=1}^{M_i} \beta_k \bar{\eta}_k - \left(\sum_{k=1}^{M_i} \alpha_k \bar{\eta}_k\right)^2\right) \\ &\triangleq \frac{L^2}{\Delta f_i^2 \pi}\left(\sum_{k=1}^{M_i} 4\pi^2 \bar{\eta}_k(\delta_k^2 + \delta_k B_k + B_k^2/3)\right. \\ &\quad \left. - \left(\sum_{k=1}^{M_i} 2\pi\, \bar{\eta}_k(\delta_k + B_k/2)\right)^2\right). \end{aligned} \tag{23}$$

where B_i denotes the bandwidth of the i^{th} numerology. Here, δ_i is the frequency shift and obtained as $\delta_i = \Delta f_i \cdot \Delta k_i$.

Remark 1: Since each symbol is multiplied by a phase factor, the effect of these multiplications can be removed during the channel equalization at the receiver unlike in PTS. Therefore, all proposed techniques in this paper do not require any SI and can be applied in 5G-NR mixed-numerology systems with the knowledge of numerology and its parameters, which are already provided by control signaling for the receiver [21].

C. COMPLEXITY ANALYSIS

The computational complexity of the proposed methods is analyzed in terms of the number of addition and multiplication operations, and then compared with the PTS scheme. The PTS achieves an effective PAPR reduction with the computational complexity according to the W dimension and V IFFT operations. The computation of a Cooley-Tukey IFFT algorithm has $\frac{N_i}{2}\log_2(N_i)$ multiplications and $N_i \log_2(N_i)$ additions [22]. Since the PTS has V subblocks, there are $V\left(\frac{N_i}{2}\log_2(N_i)\right)$ multiplications and $V\left(N_i \log_2(N_i)\right)$ additions due to the IFFT operations. Unlike PTS, the proposed methods do not require a generation of sub-sequences or IFFT operation as shown in Fig. 2 with the red color. Therefore, the computational complexity of the proposed methods only lies in finding the optimum phase factor.

All phase rotation methods require additional calculations to find the optimum phase factors. The computational complexity of finding the optimum phase factors increases exponentially with the number of subblocks. In the PTS technique, the total number of required multiplications and additions for finding the optimum phase rotation factor can be calculated as $W^{V-1}L\,(V+1)$ and $W^{V-1}L\,(V-1)$, respectively [8]. Therefore, the total computational complexity of PTS is calculated as $V\left(\frac{N_i}{2}\log_2(N_i)\right) + W^{V-1}L\,(V+1)$ multiplications and $V\left(N_i \log_2(N_i)\right) + W^{V-1}L\,(V-1)$ additions.

Since the OFDM symbols in the L duration are multiplied by the single phase, the computational complexity of Proposed-NB has the same performance with finding optimum phase factors in the PTS method as

$$W^{I-1}L\,(I+1) \tag{24}$$

multiplications and

$$W^{I-1}L\,(I-1) \tag{25}$$

additions.

In Proposed-SB, although L_i is different for each χ_i, $L = L_i M_i$ in the mixed-numerology systems due to the multiple (M_i) IFFT operations. Therefore, every numerology has L points and it is necessary to do L multiplications and additions. Then, multiplication and addition operations are carried out for I times and $I-1$ times, respectively due to the number of numerologies in the system. Afterwards, the number of total required multiplications can be given as

$$W^{\left(\sum_{i=1}^{I} M_i\right)-1}LI \tag{26}$$

and the number of total required additions can be written by

$$\left(W^{\left(\sum_{i=1}^{I} M_i\right)-1} - 1\right)L\,(I-1)\,. \tag{27}$$

In (27), $L\,(I-1)$ additions are removed due to the existing addition operation in the 5G-NR system, which is shown in Fig. 2.

Proposed-LB significantly reduces the cost of the computational complexity of Proposed-SB. Differently than the Proposed-SB, the phase multiplication is only applied on a L_{q+1} duration for every phase search. Also, $I-1$ numerologies rather than I are included to find the optimum phase factors. In the Proposed-LB, the interesting aspect above all, the exponential complexity increment with $\sum_{i=1}^{I} M_i$ subblocks (S^{SB} in (11)) seen in Proposed-SB is transformed to the cumulative complexity increment of multiple exponential (S^{LB} in (18)) calculation while achieving location-based

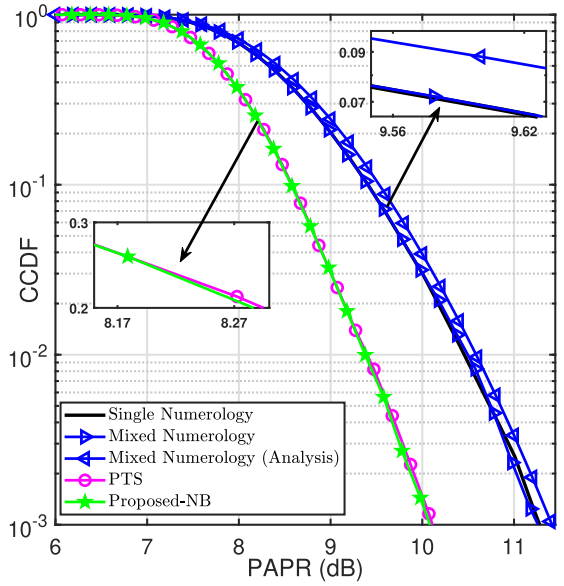

FIGURE 5. PAPR performances of conventional single&mixed-numerology and applied phase rotation approach.

PAPR calculation. Therefore, the number of total required multiplications for Proposed-LB can be given as

$$\left(\sum_{m_{q+1}=1}^{M_{q+1}} S_{m_{q+1}}^{LB}\right) L_{q+1}\,(I-1)\,, \tag{28}$$

where the minimum number of total required multiplications can be calculated as

$$\left(W^{\frac{(\sum_{i=2}^{I} M_i)-1}{M_{q+1}}}\right) L_{q+1}\,(I-1) \tag{29}$$

and the maximum number of total required multiplications can be calculated as

$$\left(M_{q+1}\left(W^{\frac{(\sum_{i=2}^{I} M_i)-1}{M_{q+1}}}-1\right)+1\right) L_{q+1}\,(I-1)\,. \tag{30}$$

The number of total required additions for Proposed-LB can be written by

$$\left(\left(\sum_{m_{q+1}=1}^{M_{q+1}} S_{m_{q+1}}^{LB}\right)-1\right) L_{q+1}\,(I-1)\,, \tag{31}$$

where the minimum number of total required additions can be calculated as

$$\left(\left(W^{\frac{(\sum_{i=2}^{I} M_i)-1}{M_{q+1}}}\right)-1\right) L_{q+1}\,(I-1) \tag{32}$$

and the maximum number of total required additions can be calculated as

$$\left(M_{q+1}\left(W^{\frac{(\sum_{i=2}^{I} M_i)-1}{M_{q+1}}}-1\right)\right) L_{q+1}\,(I-1)\,. \tag{33}$$

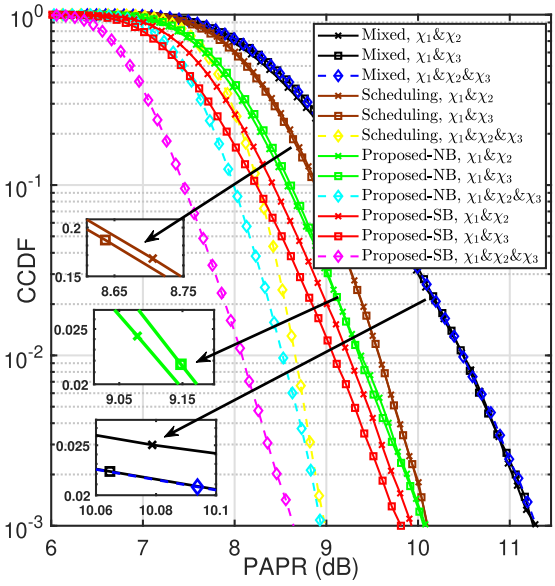

FIGURE 6. Comparison between conventional mixed numerologies, numerology scheduling, and proposed methods for different scenarios.

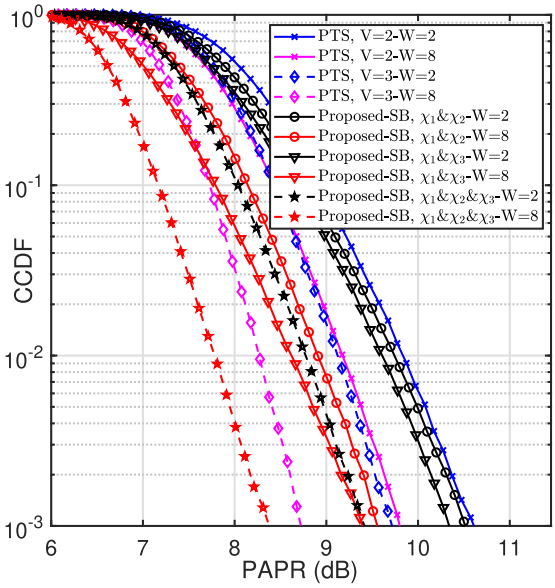

FIGURE 7. Impact of the W and comparison between PTS technique and Proposed-SB for mixed-numerology scenarios.

IV. NUMERICAL RESULTS

In this section, the simulation results are obtained to evaluate the PAPR performances. The evaluation is done with the CCDF curves and the complexity analysis. The scenarios for χ_1, χ_2, and χ_3 are taken into consideration with the $\Delta f_1 = 15$ kHz, $\Delta f_2 = 30$ kHz, and $\Delta f_3 = 60$ kHz, respectively [2]. Accordingly, $N_1 = 256$, $N_2 = 128$, and $N_3 = 64$ are chosen for the selected numerologies with the same order. The CP ratio with $1/16$ is set in OFDM system and the LCM length is set as $L = 272$. The oversampling rate is considered as 4 to approximate the discrete time-domain signals as continuous time-domain signals [11]. The bandwidth (B) is equally shared for the numerologies. The size of the phase

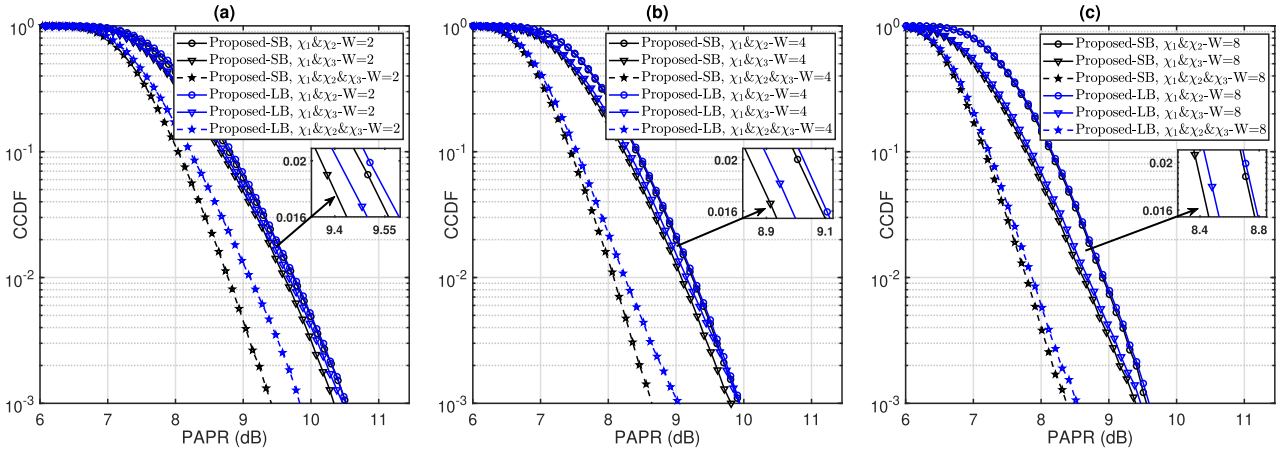

FIGURE 8. PAPR performances for the sub-optimal method Proposed-LB and the optimal method Proposed-SB for different mixed-numerology scenarios with (a) $W = 2$, (b) $W = 4$, and (c) $W = 8$.

factor is selected as $W = \{2, 4, 8\}$. 10^5 LCM symbols are generated randomly with QPSK constellations in the Monte Carlo simulations. The same symbol length is used for the performance evaluation of single or mixed numerologies and the same number of parallel sub-blocks in the time domain are considered for different methods evaluated. Therefore, PTS is set to $V = 2$ against the proposed methods setups for $\chi_1\&\chi_2$, $\chi_1\&\chi_3$ ($I = 2$) and $V = 3$ against $\chi_1\&\chi_2\&\chi_3$ ($I = 3$) scenarios. Also, the adjacent segmentation scheme in the frequency domain [22] is used for the subblocks partitioning in all methods.

The CCDF performance of PTS and proposed methods with the parameters of $W = 4$, $V = 2$, and $\chi_1\&\chi_2$ are compared to the conventional single and mixed-numerology OFDM systems in Fig. 5. The scenarios of χ_1 and $\chi_1\&\chi_2$ are considered for the single and mixed-numerology systems, respectively. As seen from Fig. 5, single and mixed numerology scenarios have similar PAPR performance that matches with the mixed-numerology analytical result. The simulation results show that Proposed-NB performs similarly to PTS due to the having same phase rotation multiplication.

Figure 6 shows the simulation results of proposed methods with $W = 4$ and conventional mixed-numerology systems for different scenarios. All conventional mixed numerologies have similar PAPR performances. Numerologies with different CP lengths do not change the PAPR performances. As a benchmark for PAPR reduction in mixed numerologies, the numerology scheduling presented in [15] is also considered. The proposed methods have a better performance than the numerology scheduling technique. Proposed-SB gives the best PAPR performance. This is because Proposed-SB enables the application of multiple phase factors for the different symbols on the L duration. Also, $\chi_1\&\chi_3$ has a better performance than $\chi_1\&\chi_2$ scenario for Proposed-SB due to a better phase adjustment with more OFDM symbols in the L duration. However, for Proposed-NB method in $I = 2$ scenarios, the use of different numerologies does not affect the performance since a single phase factor is applied to the concatenated OFDM symbols for L duration. Due to the increased number of subblocks in $I = 3$ scenario, PAPR reduction at the CCDF level of 0.1% reaches about 2.45 *dB* and 2.75 *dB* with Proposed-NB and Proposed-SB, respectively.

The PAPR reduction performance of Proposed-SB compared to the PTS for various scenarios with different W values, is shown in Fig. 7. Since the phase rotation is limited with $W = 2$, the PAPR reduction compared to conventional systems is about 1 *dB* for both methods and Proposed-SB is slightly better than PTS for the 2 parallel subblocks scenarios. However, PTS with $V = 3$ and Proposed-SB with $I = 3$ reach approximately 2 *dB* in PAPR reduction. Besides, Proposed-SB shows significant performance gains compared to PTS for higher W. Also, if the number of numerologies increases, Proposed-SB performs better when W is increased. Moreover, Proposed-SB with $I = 3$ and $W = 8$ puts the best performance and reaches 8.25 *dB* PAPR. Although not included in Fig. 7 to avoid clustering of the curves, it can be observed from conjunction with Fig. 6 that proposed methods with $W = \{4, 8\}$ are better than the numerology scheduling technique, while the opposite hold true for proposed methods with $W = 2$.

Figure 8 displays the PAPR performances of the sub-optimal method Proposed-LB and the optimal method Proposed-SB for different scenarios with $W = \{2, 4, 8\}$. The Proposed-LB with $I = 2$ gives approximately the same results as with the optimum method. For the $I = 3$ scenarios, Proposed-LB with $W = 8$ enhances PAPR performance compare to lower W sizes. Furthermore, it can be observed from the comparison between Fig. 6 and Fig. 8 (b), and also Fig. 7 and Fig. 8 (a), (c) that Proposed-LB has a better performance than Proposed-NB, the numerology scheduling method, and PTS.

Lastly, the computational complexity is evaluated for different scenarios in Table 1. Proposed-NB shows impressive performance for all scenarios and numerical results fully comply with the complexity analysis under the previous section discussion. The computational complexity reduction reaches up to 55.6% for multiplication (MLP)

TABLE 1. Numerical computational complexity analysis for PAPR reduction methods.

	PTS (χ_1)		Proposed-NB		Proposed-SB				Proposed-LB				Numerology Scheduling			
Phase Size	$V=2$		$I=2$		$\chi_1\&\chi_2$		$\chi_1\&\chi_3$		$\chi_1\&\chi_2$		$\chi_1\&\chi_3$		$\chi_1\&\chi_2$		$\chi_1\&\chi_3$	
	MLP	ADD	MLP	ADD	MLP	ADD	MLP	ADD	MLP	ADD	MLP	ADD	MLP	ADD	MLP	ADD
W=2	3680	4640	1632	544	2176	816	8704	4080	306	204	172	170	5720	21080	5224	19560
W=4	5312	5184	3264	1088	8704	4080	139264	69360	636	500	372	304				
W=8	8576	6272	6528	2176	34816	17136	2228224	1113840	1256	1119	722	654				
Phase Size	$V=3$		$I=3$		$\chi_1\&\chi_2\&\chi_3$ $(I=3)$				$\chi_1\&\chi_2\&\chi_3$ $(I=3)$				$\chi_1\&\chi_2\&\chi_3$ $(I=3)$			
	MLP	ADD	MLP	ADD	MLP		ADD		MLP		ADD		MLP		ADD	
W=2	7424	8320	4352	2176	52224		34272		2598		2856		21864		89640	
W=4	20480	14848	17408	8704	3342336		2227680		21314		21042					
W=8	72704	40960	69632	34816	213909504		142605792		164360		164090					

operation and 88.2% for addition (ADD) operation with Proposed-NB compared to the conventional PTS method. Although Proposed-SB increases computational complexity performances in the majority of the scenarios, it gives less computational complexity for most of the $W = 2$ and $I = 2$ scenarios than the PTS method with χ_1, and for almost half of the scenarios than the numerology scheduling method. The computational complexity for Proposed-LB is also analyzed. S^{LB} phase searches to find sub-optimal phase rotation factors are calculated using simulation results for all mixed-numerology scenarios in Fig. 8. As expected, Proposed-LB decreases the computational complexity reaching up to 99.9% for both operations compared to the optimum approach with Proposed-SB. Moreover, Proposed-LB shows the best computational complexity performances for all $I = 2$ scenarios. The numerical results also demonstrate that Proposed-LB is a competitive method for $I = 3$ scenarios. Furthermore, Proposed-LB has a better computational complexity performance than the numerology scheduling method in most of the scenarios.

V. CONCLUSION

This paper proposes the phase rotation approach with the OFDM mixed-numerology architecture for PAPR reduction using three methods. While taking advantage of the new 5G-NR transmitter structure, there is no additional IFFT processing compared to the conventional mixed-numerology system in the proposed methods. Also, SI is not needed for signal detection at the receiver. There is a trade-off between the PAPR reduction performance and the computational complexity for Proposed-NB and Proposed-SB. Proposed-NB gives the same performance as the PTS method and requires lower computational complexity. On the other hand, Proposed-SB achieves a better PAPR reduction performance than PTS but increases the computational complexity. Also, the numerology scheduling technique as another benchmark is compared with the proposed methods and it is observed that the proposed methods can be alternatives for PAPR reduction techniques in mixed numerologies. Moreover, it is shown that the computational complexity can be decreased significantly by using a sub-optimal method with Proposed-LB. Proposed-LB satisfies the PAPR reduction performance is approximately the same as Proposed-SB in most of the scenarios and the higher size of the phase factor gives performances closer to the optimum. Besides, the computational complexity performances of Proposed-LB give the best performances in most of the scenarios. The significance of the proposed methods lies in the fact that they fully support the existing 5G-NR multi-numerology communication standards. Also, in order to be able to respond better to future applications and users' needs, new services with a wide variety of numerologies will be utilized in beyond 5G compared to the current three services in 5G-NR. An increase in the number of numerologies improves the PAPR performances with the proposed methods. Therefore, they promise a long-term solution for PAPR reduction beyond 5G. One future direction might be the study of determining the optimum way of combining the various PAPR reduction techniques with our proposed methods, which can lead to more efficient and effective PAPR reduction. Also, developing an advanced sub-optimal algorithm that can terminate the phase search once the predetermined PAPR threshold is reached can reduce the computational complexity for PAPR reduction even further while maintaining a high level of performance.

ACKNOWLEDGMENT

The authors would like to thank Muhammad Sohaib J. Solaija for his valuable suggestions.

REFERENCES

[1] A. A. Zaidi, R. Baldemair, H. Tullberg, H. Bjorkegren, L. Sundstrom, J. Medbo, C. Kilinc, and I. Da Silva, "Waveform and numerology to support 5G services and requirements," *IEEE Commun. Mag.*, vol. 54, no. 11, pp. 90–98, Nov. 2016.

[2] *General Aspects for User Equipment (UE) Radio Frequency (RF) for NR*, document TR 38.817 V16.3.0, Release 16, 3GPP, 2021.

[3] D. Wulich, "Definition of efficient PAPR in OFDM," *IEEE Commun. Lett.*, vol. 9, no. 9, pp. 832–834, Sep. 2005.

[4] Y. Rahmatallah and S. Mohan, "Peak-to-average power ratio reduction in OFDM systems: A survey and taxonomy," *IEEE Commun. Surveys Tuts.*, vol. 15, no. 4, pp. 1567–1592, 4th Quart., 2013.

[5] Y.-C. Wang and Z.-Q. Luo, "Optimized iterative clipping and filtering for PAPR reduction of OFDM signals," *IEEE Trans. Commun.*, vol. 59, no. 1, pp. 33–37, Jan. 2011.

[6] I. P. Nasarre, T. Levanen, K. Pajukoski, A. Lehti, E. Tiirola, and M. Valkama, "Enhanced uplink coverage for 5G NR: Frequency-domain spectral shaping with spectral extension," *IEEE Open J. Commun. Soc.*, vol. 2, pp. 1188–1204, 2021.

[7] D.-W. Lim, J.-S. No, C.-W. Lim, and H. Chung, "A new SLM OFDM scheme with low complexity for PAPR reduction," *IEEE Signal Process. Lett.*, vol. 12, no. 2, pp. 93–96, Feb. 2005.

[8] Y. A. Jawhar, L. Audah, M. A. Taher, K. N. Ramli, N. S. M. Shah, M. Musa, and M. S. Ahmed, "A review of partial transmit sequence for PAPR reduction in the OFDM systems," *IEEE Access*, vol. 7, pp. 18021–18041, 2019.

[9] T. K. Nguyen, H. H. Nguyen, J. E. Salt, and C. Howlett, "Optimization of partial transmit sequences for PAPR reduction of OFDM signals without side information," *IEEE Trans. Broadcast.*, vol. 69, no. 1, pp. 313–321, Mar. 2023.

[10] Y. Lu, F. Hu, L. Jin, J. Liu, and G. Zhang, "Continuous unconstrained PSO-PTS strategy to maximize HPA energy efficiency for FBMC-OQAM systems," *IET Commun.*, vol. 17, no. 5, pp. 614–631, Mar. 2023.
[11] S. Gokceli, T. Levanen, J. Yli-Kaakinen, T. Riihonen, M. Renfors, and M. Valkama, "PAPR reduction with mixed-numerology OFDM," *IEEE Wireless Commun. Lett.*, vol. 9, no. 1, pp. 21–25, Jan. 2020.
[12] S. Gökceli, T. Levanen, T. Riihonen, J. Yli-Kaakinen, A. Brihuega, M. Turunen, M. Renfors, and M. Valkama, "Novel iterative clipping and error filtering methods for efficient PAPR reduction in 5G and beyond," *IEEE Open J. Commun. Soc.*, vol. 2, pp. 48–66, 2021.
[13] X. Liu, L. Zhang, J. Xiong, X. Zhang, L. Zhou, and J. Wei, "Peak-to-average power ratio analysis for OFDM-based mixed-numerology transmissions," *IEEE Trans. Veh. Technol.*, vol. 69, no. 2, pp. 1802–1812, Feb. 2020.
[14] X. Liu, X. Zhang, L. Zhang, P. Xiao, J. Wei, H. Zhang, and V. C. M. Leung, "PAPR reduction using iterative clipping/filtering and ADMM approaches for OFDM-based mixed-numerology systems," *IEEE Trans. Wireless Commun.*, vol. 19, no. 4, pp. 2586–2600, Apr. 2020.
[15] E. Memisoglu, A. E. Duranay, and H. Arslan, "Numerology scheduling for PAPR reduction in mixed numerologies," *IEEE Wireless Commun. Lett.*, vol. 10, no. 6, pp. 1197–1201, Jun. 2021.
[16] M. Yang, Y. Chen, and L. Du, "Multi-scale mapping algorithm for INI cancellation and a novel mixed-numerologies OFDM transceiver," *Phys. Commun.*, vol. 54, Oct. 2022, Art. no. 101849.
[17] A. Yazar and H. Arslan, "A flexibility metric and optimization methods for mixed numerologies in 5G and beyond," *IEEE Access*, vol. 6, pp. 3755–3764, 2018.
[18] S. H. Müller and J. B. Huber, "OFDM with reduced peak-to-average power ratio by optimum combination of partial transmit sequences," *Electron. Lett.*, vol. 33, no. 5, pp. 368–369, Feb. 1997.
[19] D.-W. Lim, S.-K. Heo, J.-S. No, and H. Chung, "A new PTS OFDM scheme with low complexity for PAPR reduction," *IEEE Trans. Broadcast.*, vol. 52, no. 1, pp. 77–82, Mar. 2006.
[20] A. B. Kihero, M. S. J. Solaija, and H. Arslan, "Inter-numerology interference for beyond 5G," *IEEE Access*, vol. 7, pp. 146512–146523, 2019.
[21] *NR; Physical Channels and Modulation*, document TR 38.211 V17.2.0, Release 17, 3GPP, 2022.
[22] S. Geun Kang, J. Goo Kim, and E. Kyeong Joo, "A novel subblock partition scheme for partial transmit sequence OFDM," *IEEE Trans. Broadcast.*, vol. 45, no. 3, pp. 333–338, 1999.

AHMET ENES DURANAY received the B.S. degree in electronics engineering from Gebze Technical University, Gebze, Turkey, in 2014, and the M.S. degree in electrical and computer engineering from Altinbas University, Istanbul, Turkey, in 2018. He is currently pursuing the Ph.D. degree with Istanbul Medipol University, Istanbul. He is also a member of the Communications, Signal Processing, and Networking Center (CoSiNC), Istanbul Medipol University. His research interests include interference management, non-terrestrial networks (NTNs), centralized radio access networks (C-RAN), peak-to-average power ratio (PAPR) reduction, and mobility management for 5G and beyond radio access technologies.

EBUBEKIR MEMISOGLU received the B.S. degree in electrical and electronics engineering from Istanbul University, in 2016, and the M.Sc. degree in telecommunications engineering from Istanbul Technical University, Istanbul, Turkey, in 2019. He is currently pursuing the Ph.D. degree with the Communications, Signal Processing, and Networking Center, Istanbul Medipol University, Istanbul. His current research interests include wireless communications, waveform design, index modulation, and integrated sensing and communication.

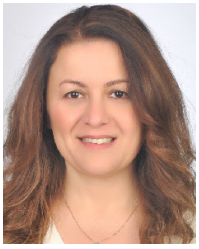

BAŞAK ÖZBAKIŞ received the B.S. degree from the Department of Electrical and Electronics Engineering, Dokuz Eylül University, Turkey, in 2001, and the M.S. and Ph.D. degrees from the Izmir Institute of Technology (IYTE), in 2004 and 2012, respectively. She was a Research Assistant with IYTE, from 2001 to 2011. In 2012, she was with the Research and Development Department, Vestel. She has been an EMC Engineer, Project Specialist, and IP Specialist. She is currently involved in standard essential patents related to Wi-Fi and 6G. She is representing Vestel as a Voter Member in IEEE 802.11 WLAN and as a delegate in 3GPP standard organizations.

HÜSEYIN ARSLAN (Fellow, IEEE) received the B.S. degree from Middle East Technical University (METU), Ankara, Turkey, in 1992, and the M.S. and Ph.D. degrees from Southern Methodist University (SMU), Dallas, TX, USA, in 1994 and 1998, respectively.

From January 1998 to August 2002, he was with the Research Group, Ericsson, where he was involved with several projects related to 2G and 3G wireless communication systems. From August 2002 to August 2022, he was a Professor with the Department of Electrical Engineering, University of South Florida. In December 2013, he joined Istanbul Medipol University and founded the Engineering College, where he has been the Dean of the School of Engineering and Natural Sciences. In addition, he was a part-time Consultant for various companies and institutions, including Anritsu Company and the Scientific and Technological Research Council of Turkey. He conducts research in wireless systems, with an emphasis on the physical and medium access layers of communications. His current research interests include 6G and beyond radio access technologies, physical layer security, interference management (avoidance, awareness, and cancellation), cognitive radio, multi-carrier wireless technologies (beyond OFDM), dynamic spectrum access, co-existence issues, non-terrestrial communications (high altitude platforms), joint radar (sensing), and communication designs. He was collaborating extensively with key national and international industrial partners and his research has generated significant interest in companies, such as InterDigital, Anritsu, NTT DoCoMo, Raytheon, Honeywell, and Keysight Technologies. Collaborations and feedback from industry partners have significantly influenced his research. In addition to his research activities, he has also contributed to wireless communication education. He has integrated the outcomes of his research into education which lead him to develop a number of courses with the University of South Florida and Istanbul Medipol University. He has developed a unique Wireless Systems Laboratory course (funded by the National Science Foundation and Keysight Technologies) where he was able to teach not only the theory but also the practical aspects of wireless communication systems with the most contemporary test and measurement equipment.

Dr. Arslan is a member of the Turkish Academy of Sciences and a Distinguished Lecturer. He has served as the general chair, the technical program committee chair, the session and symposium organizer, the workshop chair, and the technical program committee member for several IEEE conferences. He is currently a member of the editorial board of IEEE Surveys and Tutorials and Sensors Journal. He has also served as a member of the editorial board for IEEE Transactions on Communications, IEEE Transactions on Cognitive Communications and Networking (TCCN), and several other scholarly journals by Elsevier, Hindawi, and Wiley Publishing.